Kinetic pathways of diffusion and solid state reactions in nanostructured thin film systems

Beke[1], Dezső, L.; Langer[1], Gábor,A.; Molnár[1], Gábor; Erdélyi[1], Gábor; Katona[1], Gábor, L.; Lakatos[1], Ákos; Vad[2], Kálmán,

[1]*Department of Solid State Physics, University of Debrecen, 4010 Debrecen, PoBox 2. Hungary*

[2]*Nuclear Research Institute of the Hungarian Academy of Sciences. Debrecen*

dbeke@delfin.unideb.hu

Kinetic pathways of diffusion and solid state reactions in nanostructured thin film systems

Mass transport and solid state reactions in nanocrystalline thin films is reviewed. It is illustrated that diffusion along different grain boundaries, GB, can have important effects on the overall intermixing process between two pure films. These processes can be well characterized by a bimodal GB network, with different (fast and slow) diffusivities. First the atoms migrate along fast GBs (triple junctions) and accumulate at the film surface. These accumulated atoms form a secondary diffusion source for back diffusion along slow boundaries. Thus the GBs of the thin films can be gradually filled up with the diffusing atoms and composition depth profiles reflect the result of these processes. Similar process can be observed in binary systems with intermetallic layers: instead of nucleation and growth of the reaction layer at the initial interface, the reaction takes place in the GBs and the amount of the product phase growths by the motion of its interfaces perpendicular to the GBs. Thus, the entire layer of the pure parent films can be consumed by this GB diffusion induced solid state reaction (GBDIREAC), and a fully homogeneous product layer can be obtained.

Keywords: diffusion, solid state reactions, thin films, nanostructures

1. Introduction

The problem of solid state reactions in nanostructured thin film systems, i.e. in bilayers or multilayers with individual thicknesses of few nanometers, is still a challenging subject. If the films are nanocrystalline the mass transport along different grain boundaries, GBs, (short circuits) can have an important effect on the entire intermixing process. We have shown recently [1-5], that this process can be well characterized by a bimodal GB network with fast and slow diffusivities Furthermore, at low temperatures, during interdiffusion in binary systems where intermetallic layers can grow, it can be observed that the morphology of the formation and growth of the reaction product can be different from the usual picture observed at high temperatures, where the new

continuous phases form at the initial interface growing parallel to the initial contact surface. Indeed, it is known that at low temperatures, where bulk diffusion processes are practically frozen, even a complete intermixing of components in binary nanocrystalline couple can happen by grain boundary migrations through the volume [6,7,8]. The diffusion induced grain boundary motion, DIGM, and diffusion induced recrystallization, DIR, are the examples of such kind of GB motions. During DIR new grains are formed with composition discontinuously different from the surrounding original grains, while in DIGM the composition of the zone left behind the sweeping boundary is also higher but has not such a well defined value. Although still there are discussions in the literature about the role of chemical driving forces [9], it is more and more widely accepted that in both processes the driving forces are related to stress accumulation and relaxation ahead/around the moving boundary [6,10,11].

It is rather difficult to make a distinction between DIR and DIGM experimentally (see e.g. [12]). DIR was mainly investigated in binary systems with wide mutual solubility range above either the miscibility gap or the critical temperature of ordering (e.g. in Cu/Pd [12], Au/Cu [13], Ag/Pd [14], Ni/Cu [9,15]). Even a model intrepreting DIR was developed for such systems in [6].

Recently, for instance in [16] and [17], intermixing in nanocrystalline systems with reactive diffusion was investigated at low temperatures where different intermetallic phases were formed. It was observed in Cu/Pd system that the interface between the two layers remained clearly visible (see the TEM picture in Fig. 9b of [17]) at 473K, but the selected area diffraction patterns in TEM clearly indicated the presence of the PdCu phase. After heat treatments at 533 K, an extensive intermixing had taken place, accompanied by grain boundary migration, grain growth, and formation of phases PdCu and Cu_3Pd.

In this paper, by re-examining the discussions of the results of [3] and [17] (on Co/Si and Cu/Pd systems, respectively) and by using also our results obtained in Pd/Cu [18] as well as for Pt/(Ag)/Fe systems [19], general features of low temperature reaction layer formations are summarized. This process can be called Grain Boundary Diffusion Induced Reaction layer formation (GBIREAC) and can lead to formation of a completely reacted nanocrystalline thin film into A_nB_{1-n} intermetallic layer, where n depends on the initial film thicknesses and grain sizes.

2. Objectives and methods

Since this is a review paper the preliminary results of other authors and the experimental observations from our laboratory will summarized first and then a comprehensive picture will be given about the possible kinetic pathways of diffusion and solid state reactions in nanostructured thin film systems. In our investigations the methods used were computer simulations and the experiments were based mainly on nanoscale depth profiling of thin film bilayers by Secondary Neutral Mass Spectroscopy and TEM [1-5, 18 and 19].

3. Summary of Results

It was shown more recently in our Laboratory [1,2,3] that having a substrate/diffusant/thin-film/cap-layer structure (the thin film was typically several 10 nm thick, with grain sizes of the same order of magnitude; the refractory metal cap layer was used just to avoid the oxidation), first the diffusant atoms migrated very fast across the thin film and segregated at the film/cap-layer interface. The accumulated atoms at the film/cap layer interface formed a secondary diffusion reservoir and atoms diffused back to the thin layer. Thus the thin film was gradually filled up with the diffusing atoms and composition depth profiles, determined by Secondary Neutral Mass Spectroscopy (SNMS), showed a maximum at the cap layer-thin film interface. These

observations were interpreted by supposing a bimodal grain boundary network with different (fast and slow) diffusivities. The appearance of the diffusing atoms at the cap layer interface can be used as a tool to determine the grain boundary diffusivity along the fast boundaries (triple junctions). Because of the fast boundaries were saturated in the first stage of the process, the back-diffusion took place along the low-diffusivity boundaries only. Nevertheless, the observed grain boundary diffusion phenomena can be classified as C-type diffusion, i.e. the volume diffusion penetration depth was shorter than the GB width. From the overall impurity content inside the film, the segregation can also be estimated in phase separating systems from the SNMS depth-profiling, if the bulk solubility is low and the GB density is known [1].

Numerical simulations of C-type GB diffusion in thin films with a bimodal structure confirmed that the interpretation of the result depicted above is reasonable [4,5]. In order to estimate roughly the GB diffusion data we determined the fast diffusivity using the first appearance method. In addition both (slow and fast) diffusivities were also estimated from fitting numerical solutions obtained in [4] too.

Fig. 1 shows the composition profile of Ta in the nanocrystalline-Cu layer (W cap layer was used). Note the Ta peak at the W/Cu interface and the high overall composition of Ta in the Cu layer [1]. Similar phenomenon was observed in single crystalline Si-(111)substrate/nanocrystalline-Co(140nm)/Ta-cap-layer(10nm) system: here the Si diffused into the Co GBs [3]. Fig. 2 shows the experimental Si profile and the fitted curve as calculated from the bimodal GB diffusion model [4].

It is worth noting that in the case of Co/Si system, as it is well known, solid state reaction products are expected. This was still neglected in the evaluation of the results obtained in the Si/Co system, although the unusually high Si content (observed at longer annealing times) in the centre of Co layer was already attributed to a possible compound

layer formation along GBs of Co in [3] and [5]. Thus, the above description can be applicable at shorter annealing times only.

Figure 3 illustrates what happens if the annealing time is longer. It can be seen that at 583 K still there is a Si segregation at the cap layer interface (the Si content here is about 60%!) and in the centre of the Co layer the Si composition is about 20%. Furthermore on the Si side there is a shoulder in the composition profiles indicating the formation of a Si rich layer (Si reach Si_2Co compound): this layer growths at the expense of the Si. (It can be expected that, since there are no GBs in the Si this layer forms with interfaces parallel with the initial Si interface: unfortunately no TEM picture were published in [3]). On the other hand, at 623K for 24h (Fig. 3b) the average concentration of the whole sample corresponds to the 1:4 Co:Si composition, with the exception of the region of the original Co/Ta interface: in this region the Co/Si ratio is about 1:2 ($CoSi_2$). It is worth mentioning that from the SNMS profiles alone it was not possible to draw equivocal conclusion about the structure of possible phases formed. For example the broad layer of 1:4 effective Co/Si ratio (Fig. 3b) can be the result of an intensive intermixing leading to a gradual impoverishment of the expanding $CoSi_2$ layer (see the length scale, which indicates that the width of the reaction zone now is about of the double of the initial Co layer).

We have also carried out systematic investigations in other systems with reaction layer formation during diffusional homogenization i.e. in Pd/Cu [18] and Pt/Fe as well as Pt/Ag/Fe[19] systems too.

Figure 4 shows our results obtained at 523 K in Pd(30nm)/Cu(50nm) system deposited onto MgO substrate [18]. It can be clearly seen that - after a fast stage of filling up the GBs - there is a gradual increase in the average composition in the centre of both films which can be interpreted by the motion of interfaces bordering the new phases formed

along the GBs (figure 4). These interfaces move perpendicular to the initial GB leaving behind the reaction layer. This is similar to a diffusion induced re-crystallization, DIR, process, when the GB sweeps and leaves behind an alloyed region and can be called as "GB diffusion induced reaction layer formation", GBDIREAC. Using x-ray diffraction and transmission electron microscopy (TEM), Chakraborty et al. [17] convincingly proved that under the same conditions, in Pd/Cu bilayer film, intermetallic phases (Cu_3Pd and CuPd) have been formed. In their TEM micrograph no reaction layer could be detected in the vicinity of the original interface (at 498 and 523 K up to 6 and 3 h, respectively) and selected area electron diffraction clearly indicated the presence of the CuPd phase. The similarity of their depth profiles obtained at 523 K and the one shown in figure 4b is remarkable. It is worth mentioning that the formation and normal growths of a reaction layer can be usually detected in the SNMS concentration–depth profiles as well (see e.g. [20], where the growth of a NiSi phase between Ni and amorphous Si was followed by SNMS technique). However – also in accordance with [17] - we did not observe the effects of such reaction layer in our depth profiles. Our experimental findings can be explained in a way that instead of nucleation and growth of a product layer, parallel to the original interface, the compound phase is formed by means of GBDIREAC. By means of this mechanism, the high concentration regions with compositions close to the stoichiometric composition may develop in GBs and can grow consuming the parent phase. The grain boundary network in thin films, even at low temperatures, is able to supply enough material to reach a complete homogenization or phase formation in the whole volume of the film. Figure 5 illustrates schematically the effect of GBDIREAC on the entire composition profile inside the films.

It is worth noting that in [17] and [21] although even the bulk interdiffusion coefficients were estimated from the near interface region, we prefer the explanation offered above

(see also our estimations for the bulk diffusivities in [19], which showed that the volume diffusion was frozen in the above temperature range).

Furthermore, while in [18] we have concentrated on the first stages of the intermixing as illustrated above, the result obtained at longer annealing times are also very interesting. Indeed, at later stages the average compositions inside both initial layers increases and the final result is an almost homogeneous 50/50 CuPd compound formation (figure 4c). It is important noting that the final result of such kind of low temperature homogenization can be different depending on the initial grain size, the ratio of the initial film thicknesses, the temperature and stress distribution influenced by the substrate too, in accordance with the predictions as described in [7]. Indeed as it is illustrated in figure 6 it is also possible to arrive at a different homogeneous state by changing the substrate (to Si (001) with native SiO_2) and the annealing temperature (to 583K). Here the final state corresponds to the Cu_3Pd compound.

Similar phenomena were observed in Pt(15nm)/Fe(15nm) as well as in Pt(15nm)/Ag(10nm)/Fe(15nm) systems [19]. It can be seen in figure 7 that at 613 K there is a mutual penetration of the elements into each other in the Pt(15nm)/Ag(10nm)/Fe(15nm) film. First (at t= 0.5 h) there is an intensive intermixing between the Pt and Ag: this is similar to the intermixing between Pd and Cu in Pd/Cu samples. Furthermore, there is a strong segregation of Pt at the Ag/Fe interface as well as a considerable penetration of Pt into the Fe layer. On the other hand, there is practically no Fe penetration into the Ag and Pt. Furthermore the Ag strongly segregates at the free surface of Pt. At 1 hour annealing time the Pt and Ag layers are strongly intermixed and at the same time there is an increased penetration of Pt into the Fe and the Pt segregates at the Fe/Si interface. At longer annealing times (t=1.5h, 3.25h and 4h) the compositions of all the three elements gradually level off and the final state is the

almost homogeneous reaction layer with Ag segregation at the free surface. There is an indication that at intermediate annealing times (t=1.5 h and 3.25 h) the PtAg intermediate phase has also been formed (with about 50%-50% composition).

Figure 8 illustrates that - similarly to the observations in the Pd/Cu system - how the initial conditions influence the time evolutions: it can be seen, by comparison with figure 7e, that the two SNMS depth profiles taken on two samples from the same sample set and annealed under identical conditions can be different. The degree of homogenization is different most probably because of slight differences in the gain structures of the films.

The TEM pictures, taken at two different parts on the Pt(Ag)/Fe sample annealed at 613 K for 1.5 hours, are shown in figure 9. It can be seen, in accordance with figure 7d, that

i) There are no continuous reaction layers at the interfaces,

ii) The lower one third of the sample (lying on the side of the original free surface) consists of two regions of a bit different brightness; both seem to be not fully homogeneous but (at least in some parts) rather consist of a mixture of two differently bright areas,

iii) The remaining two-third seems to be more homogeneous nanocrystalline film with some bright areas around several grain boundaries in the region closer to the original Ag/Fe interface.

Finally, it is worth mentioning that there are other evidences in the literature about the reaction layer formation (intermetallic phases) along GBs during interdiffusion. For instance at was shown recently [22] that in the Cu/Sn system after heat treatment at room temperature for 5 days the Sn grain boundaries were decorated by the

intermetallic layer (see figure 2 in [22] where the pure Sn layer was removed by selective etching).

4. Conclusions

Diffusion and solid state reactions in nanocrystalline thin films have the following general features:

- First there is a fast diffusion along the fastest GB's (triple-junctions)
    - Accumulation at the top most surface
    - From this secondary source there is a back diffusion along slower boundaries
    - Measurable increase of the average concentration of the diffusant in the centre of the film: the average concentration is higher than the value supposing completely saturated GBs
    - The formation of the reaction product takes place along the GBs filled up with the diffusant and no planar reaction front forms at the initial interface
    - The formation of the reaction layers around the GBs takes place by interface process: the GBs move perpendicular to the initial GB leaving behind the reaction layer. This is similar to a diffusion induced re-crystallization, DIR, process, when the GB sweeps and leaves behind an alloyed region and can be called as GBDIREAC.
    - As a result of the above process finally even a fully reacted compound layer can be formed from the initial bilayered structure by GB/interface diffusion alone. This way of the reaction layer formation is different from the usual solid state reactions observed at higher temperatures where a compact reaction layer forms and grows parallel with the initial interface (with contributions from bulk diffusion as well).

- Some intermixing of the traditional reaction layer formation and the GBDIREAC can also take place if the GB diffusion coefficients of B in the A film are not too much faster than the bulk diffusion of A in B. In this case first a GBDIREAC takes place in A and then a classical reaction layer can be formed in B (see figure 3a and 3b).

4. Acknowledgments

The project was funded by OTKA, Grant No. 80126 and by TÁMOP 4.2.1/B-09/1/KONV-2010-0007 project which is implemented through the New Hungary Development Plan co-financed by the European Social Fund and the European Regional Development Fund, Hungary

References

[1] A. Lakatos, G. Erdelyi, G.A. Langer, L. Daroczi, K. Vad, A. Csik, A. Dudas, D.L. Beke, Vacum, 84 (2010) p.953

[2] A. Lakatos, A. Csik, G.A. Langer, G. Erdelyi, G.L. Katona, L. Daroczi, K. Vad, J. Toth, D.L. Beke, Vacuum, 84 (2010) p.130

[3] A. Lakatos, G. Erdelyi, A. Makovec, G. A. Langer , A.Csik , K. Vad, D. L. Beke, Vacuum, 86 (2012) p.724

[4] A. Makovecz, G. Erdelyi, D.L. Beke, Thin Solid Films 520 (2012) p. 2362

[5] D.L Beke, A.Lakatos, G. Erdelyi, A. Makovecz, G. A. Langer, L. Daroczi, K. Vad, A.Csik, Defect and Diffusion Forum 312-315 **(**2012) p.1208

[6] G. Schmitz, D. Baither, M.Kasparzak, T.H. Kim, B.Krause, Scripta Mat. 63 (2010) 484-487

[7] V.M. Koshevich, A.N. Gladkikh, M.V. Karpovskyi, V.N. Klimenko, Interface Science, 2 (1994) 261-270

[8] L.N. Paritskaya. Yu. Kaganovskii, V.V. Bogdanov, Solid State Phenomena, Vols.101-102 (2005) 123-130

[9] M. Kajihara Scripta Mater. 54 (2006) 1767

[10] O.Penrose, Acta Mater. 52 (2004) 3901

[11] D.N.Yoon, Rev.Mater.Sci. 19 (1989) 43

[12] S.Inomata, M.O.M. Kajihara, J Mater. Sci. 46 (2011) 2410-1421

[13] F. Hartung, G. Schmitz, Phys. Rev. B64 (2001) 245418

[14] D. Baiter, T.H. Kim, G.Schmitz, Scripta Mater. 58 (2008) 99

[15] J. Sheng, U. Welzer, E.J.Mittemeijer, Z. Kristallogr. Suppl. 30 (2009) 247

[16] T. Takenaka, M. Kajihara, Material Trans. 47 (2006) 822-828

[17] J. Chakraborty, U. Welzer, E.J. Mittemeijer, J of Appl. Phys. 103 (2008) 113512

[18] G. Molnár, G. Erdélyi, G. Langer, D.L. Beke, A. Csik, M. Kis-Varga, A. Dudás, submitted to Vacuum.

[19] G.L. Katona, I. Vladimirsky, I.M. Makogon, S.I Sidorenko, L. Daróczi. A. Csik, G. Beddies, M. Albrecht. D.L. Beke, to be published

[20] A. Lakatos, G. A. Langer, A. Csik, C. Cserhati, M. Kis-Varga, L. Daroczi, G. L. Katona, Z. Erdélyi, G. Erdelyi, K. Vad,and D. L. Beke, Appl. Phys. Letters **97** (2010) 233103

[21]] J. Chakraborty, U. Welzer, E.J. Mittemeijer, Thin Solid Films, **518**, (2010) 2010

[22] N. Jadhav, E. J. Buchovecky, L. Reinbold, S. Kumar, A. F. Bower, E. Chason, IEEE TRANSACTIONS ON ELECTRONICS PACKAGING MANUFACTURING**, 33/3** (2010) 183

Figure captions

Fig. 1. Ta composition profile in the Cu after different annealing times at 593K in W(12nm)/Cu(25nm)/Ta(10nm)/Si(111)substrate system [1]

Fig. 2. Si composition profiles in the Co layer after different annealing times at 583 K (a) and the measured and fitted profile corresponding to the heat treatment at 573 K for 5h [2,3] (see also the text)

Fig. 3 Si composition profiles in the Co layer after longer annealing times at two different temperatures (a) at 583K for 24h, b) at 623K for 24h) [3]

Fig. 4 Composition versus sputtering time profiles for as deposited (on MgO substrate) (a) and annealed Pt(30nm)/Cu(50nm) films at 523 K for 1h (b) and 4h (c), respectively.

Fig.5 Diffusion and formation of reaction layers around GBs in an A/B thin film, schematically. A and B are blue and green and the reaction layers are in light blue and brown, respectively. The composition profiles obtained by depth profiling reflect the average values along vertical lines in the figure.

Fig. 6 Composition versus sputtering time profile for sample deposited on Si(001) substrate and heat treated at 583 K for 1h.

Fig. 7 Composition versus sputtering time profiles for Pt(15nm)/Ag(10nm)/Fe(15nm) samples after different annealing times at 613 K.

Fig. 8. Composition versus sputtering time profiles for an another piece of the same sample set after the same annealing as it is shown in figure 7e

Fig. 9 TEM pictures taken at two different parts of the Pt(15nm)/Ag(10nm)/Fe(15nm) sample heat treated at 613 K for 1.5 h.

Fig.1

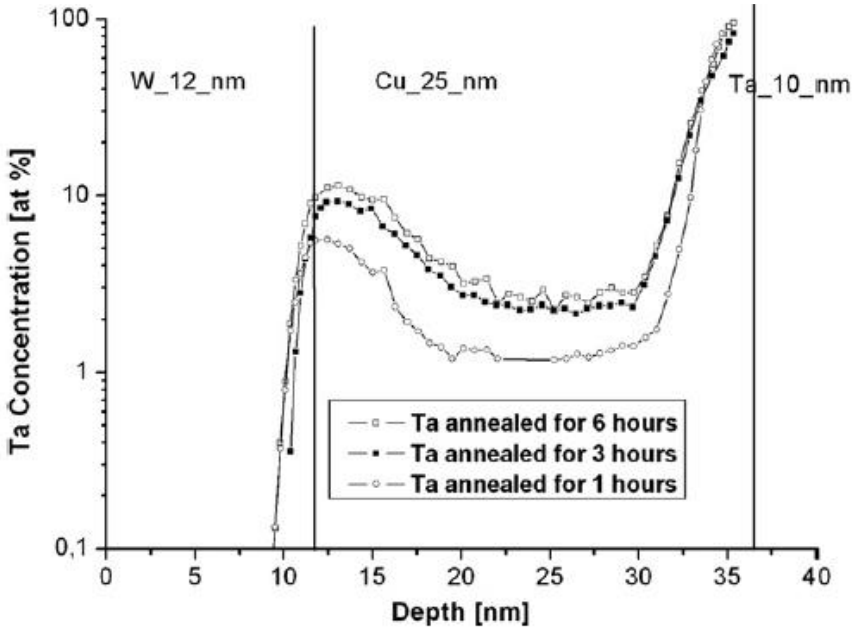
W_12_nm
Cu_25_nm
Ta_10_nm
Ta annealed for 6 hours
Ta annealed for 3 hours
Ta annealed for 1 hours
Ta Concentration [at %]
Depth [nm]
100
10
1
0,1
0
5
10
15
20
25
30
35
40

Fig. 2.

a)

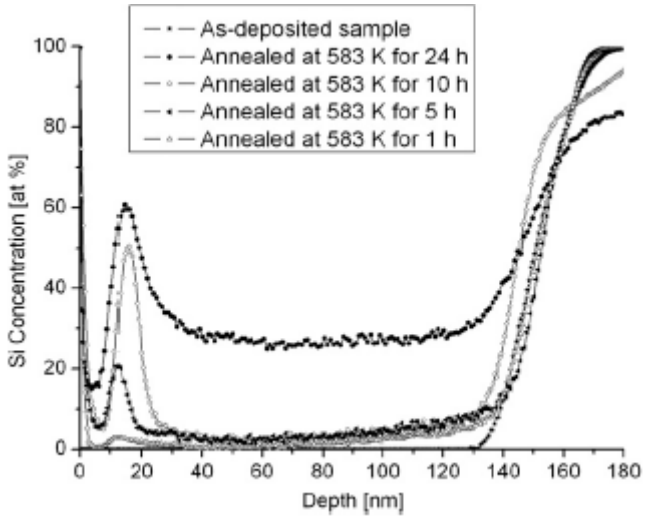
As-deposited sample
Annealed at 583 K for 24 h
Annealed at 583 K for 10 h
Annealed at 583 K for 5 h
Annealed at 583 K for 1 h
Si Concentration [at %]
Depth [nm]
0
20
40
60
80
100
120
140
160
180

b)

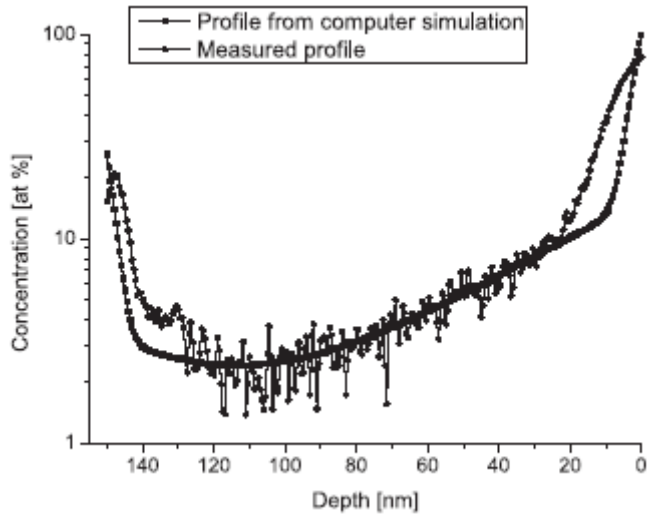
Profile from computer simulation
Measured profile
Concentration [at %]
Depth [nm]
1
10
100
140
120
100
80
60
40
20
0

Fig. 3.

a)

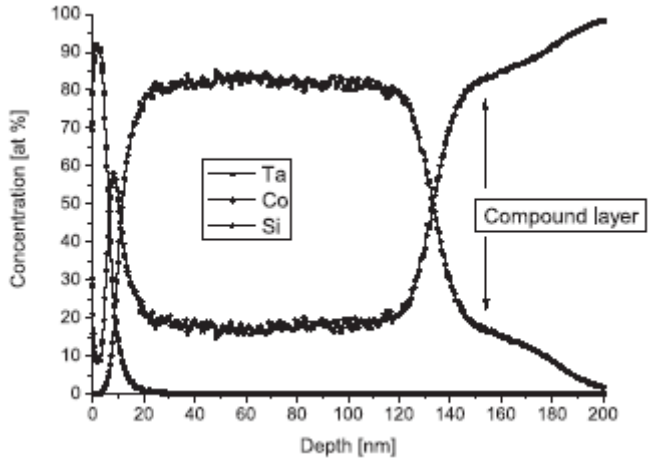
Concentration [at %]
Depth [nm]
Ta
Co
Si
Compound layer

b)

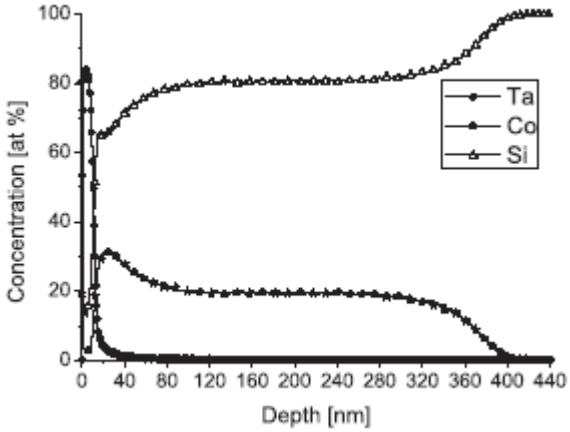
Concentration [at %]
Depth [nm]
Ta
Co
Si

Fig. 4.

a)

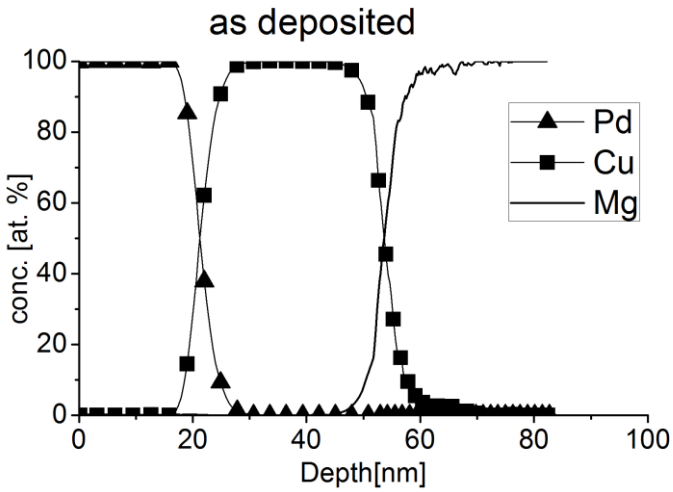
as deposited
Pd
Cu
Mg
conc. [at. %]
Depth[nm]
0
20
40
60
80
100

b)

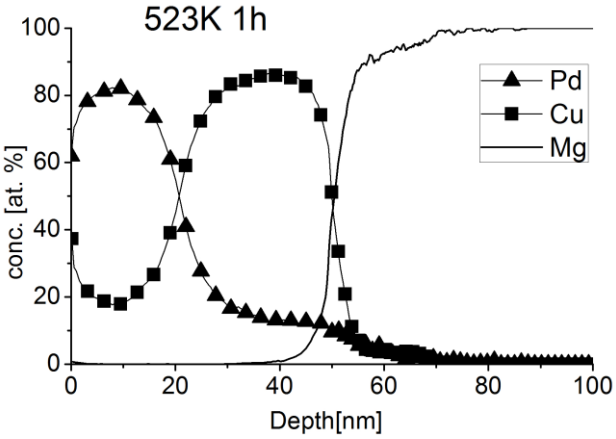
523K 1h
Pd
Cu
Mg
conc. [at. %]
Depth[nm]
0
20
40
60
80
100

c)

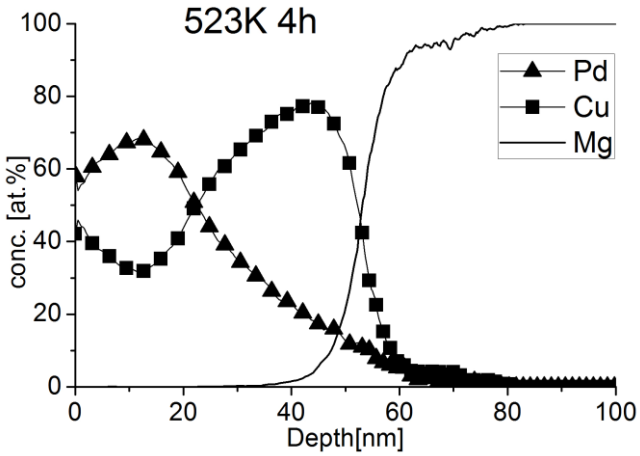
523K 4h
Pd
Cu
Mg
conc. [at.%]
Depth[nm]
0
20
40
60
80
100

Fig. 5.

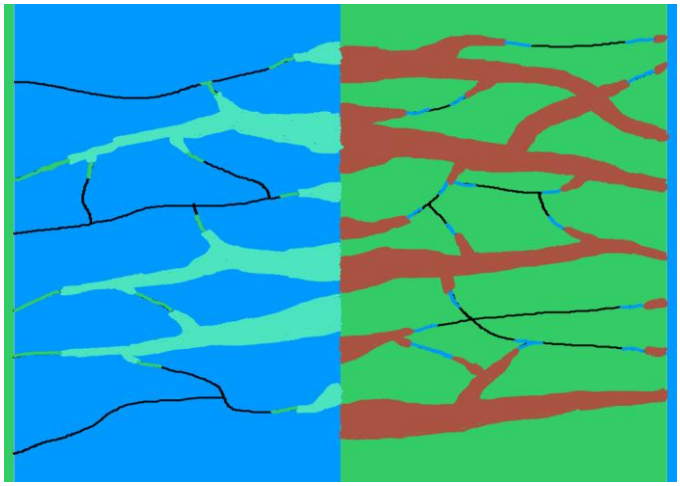

Fig. 6

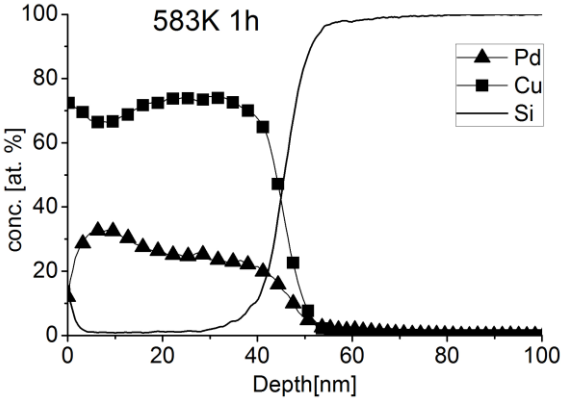

Fig. 7

a)

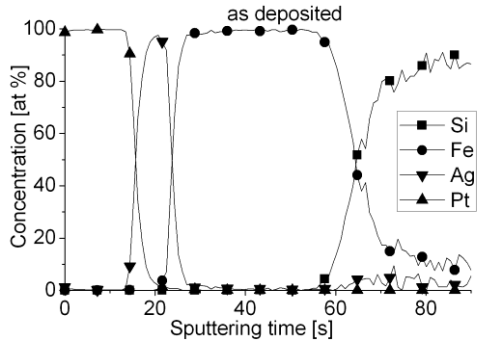
as deposited
Concentration [at %]
Sputtering time [s]
Si
Fe
Ag
Pt

b)

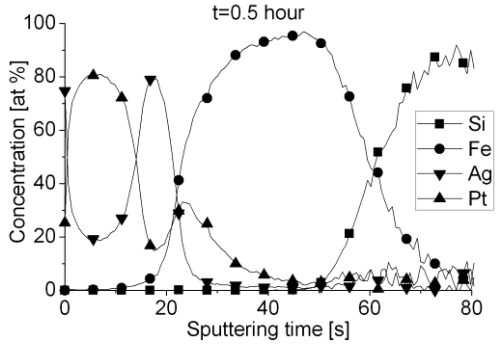
t=0.5 hour
Concentration [at %]
Sputtering time [s]
Si
Fe
Ag
Pt

c)

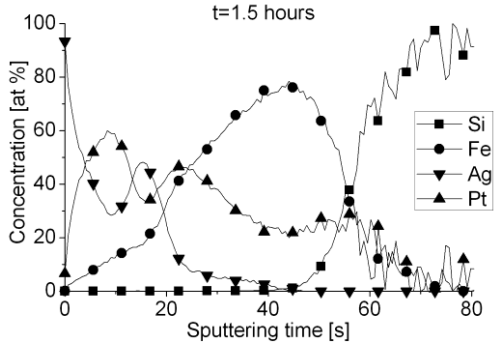
t=1.5 hours
Concentration [at %]
Sputtering time [s]
Si
Fe
Ag
Pt

d)

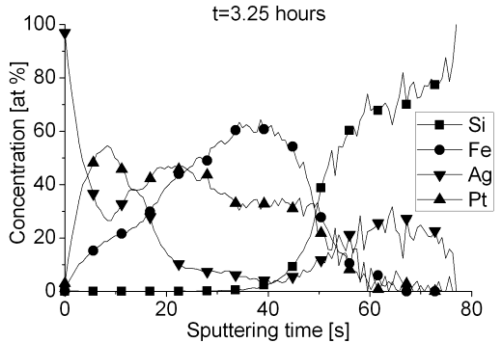
t=3.25 hours
Concentration [at %]
Sputtering time [s]
Si
Fe
Ag
Pt

e)

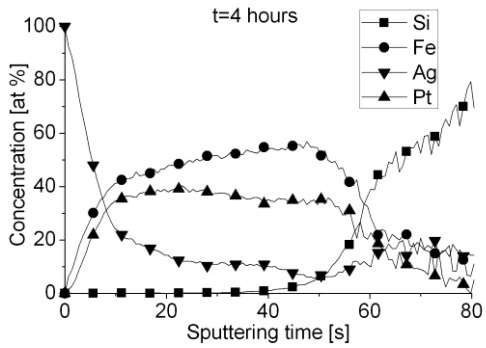
t=4 hours
Si
Fe
Ag
Pt
Concentration [at %]
Sputtering time [s]
0
20
40
60
80
100

Fig. 8

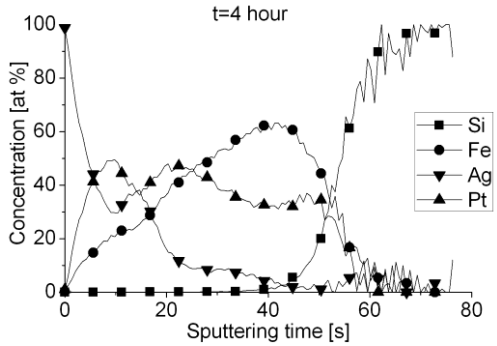
t=4 hour
Si
Fe
Ag
Pt
Concentration [at %]
Sputtering time [s]
0
20
40
60
80
100

Fig. 9